Received: 11 June 2019 | Revised: 13 July 2020 | Accepted: 15 July 2020

DOI: 10.1111/joa.13293

ORIGINAL PAPER

ANATOMICAL SOCIETY Journal of Anatomy WILEY

Body size miniaturization in a lineage of colubrid snakes: Implications for cranial anatomy

Mahdi Rajabizadeh[1,2] | Dominique Adriaens[3] | Barbara De Kegel[3] | Aziz Avcı[4] | Çetin Ilgaz[5] | Anthony Herrel[1,3,6]

[1]UMR7179 CNRS/MNHN, Département `Adaptations du vivant, Museum National d'Histoire Naturelle, Paris, France

[2]Department of Biodiversity, Institute of Science and High Technology and Environmental Sciences, Graduate University of Advanced Technology, Kerman, Iran

[3]Department of Biology, Evolutionary Morphology of Vertebrates, Ghent University, Ghent, Belgium

[4]Department of Biology, Faculty of Science and Arts, Aydın Adnan Menderes University, Aydın, Turkey

[5]Department of Biology, Faculty of Science, Dokuz Eylül University, İzmir, Turkey

[6]Department of Biology, Functional Morphology, University of Antwerp, Antwerp, Belgium

Correspondence
Mahdi Rajabizadeh, UMR7179 CNRS/MNHN, Département `Adaptations du vivant, Museum National d'Histoire Naturelle, Paris, France.
Email: khosro.rajabizadeh@gmail.com

Abstract

As body size strongly determines the biology of an organism at all levels, it can be expected that miniaturization comes with substantial structural and functional constraints. Dwarf snakes of the genus *Eirenis* are derived from big, surface-dwelling ancestors, considered to be similar to those of the sister genus *Dolichophis*. To better understand the structural implications of miniaturization on the feeding apparatus in *Eirenis*, the morphology of the cranial musculoskeletal system of *Dolichophis schmidti* was compared with that of the miniature *Eirenis punctatolineatus* and *E. persicus* using high-resolution μCT data. The gape index was compared between *D. schmidti* and 14 *Eirenis* species. Our results show a relatively increased neurocranium size and decreased maximal jaw muscle force in *E. persicus*, compared with the *D. schmidti*, and an intermediate situation in *E. punctatolineatus*. A significant negative allometry in gape index relative to body size is observed across the transition from the *Dolichophis* to *Pediophis* and *Eirenis* subgenera. However, the gape index relative to head size showed a significant negative allometry only across the transition from the *Dolichophis* to *Pseudocyclophis* subgenus. In *Dolichophis–Eirenis* dwarfing lineages, different structural patterns are observed through miniaturization, indicating that overcoming the challenge of miniaturization has achieved via different adaptations.

KEYWORDS

Dolichophis, *Eirenis*, miniaturization, morphology, myology, osteology

1 | INTRODUCTION

As body size strongly determines the biology of an organism at all levels (e.g., morphology, physiology, ecology, behavior), it can be expected that miniaturization comes with substantial structural and functional constraints (Schmidt-Nielsen, 1984; Boback and Guyer, 2003; Pyron and Burbrink, 2009). However, the fact that miniaturization evolved many times independently across the animal kingdom indicates that it also comes with benefits, such as improved predator avoidance, exploitation of alternative food resources, utilization of physically smaller niches, and attaining reproductive maturity at an earlier age (Zimkus *et al*., 2012). This convergent phenomenon is quite common across several clades of reptiles (see Hanken and Wake, 1993). In snakes, for example, dwarfism is well known in *Bitis* (Lenk *et al*., 1999), *Lampropeltis* (Pyron and Burbrink, 2009), *Leptotyphlops* (Hedges, 2008), *Tantilla* (Wilson and Mata-Silva, 2014), and *Eirenis* (Mahlow *et al*., 2013).

The genus *Eirenis* currently comprises about 24 species, classified into four subgenera (*Eirenis* Jan, 1863; *Pseudocyclophis* Boettger, 1888; *Eoseirenis* Nagy *et al*., 2003; *Pediophis* Fitzinger, 1843) (Figure 1). The genus *Eirenis* Jan, 1863 forms the sister group to big, surface-dwelling species of the genus *Dolichophis*, and are thought to represent their ancestral condition (Schätti, 1988; Schmidtler,

 © 2020 Anatomical Society

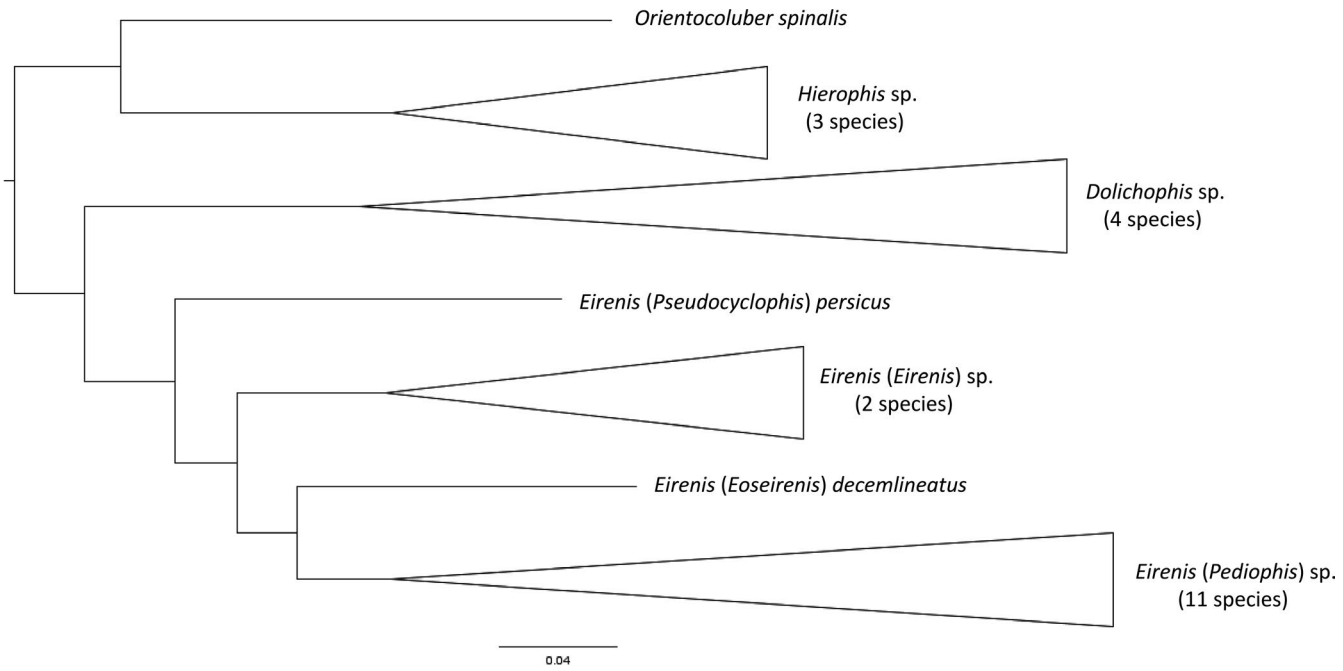

FIGURE 1 Phylogenetic relationships among the genus *Eirenis* and closely related snakes of the genera *Dolichophis* and *Hierophis* (following Figueroa *et al*., 2016). The scale bar indicates percentage of genetic variation among the taxa

1993; Schätti and Utiger, 2001; Nagy *et al*., 2003; Pyron *et al*., 2013; Figueroa *et al*., 2016; Zaher *et al*., 2019).

Eirenis is distributed across western Asia, southeastern Europe, and northeastern Africa (Schmidtler and Schmidtler, 1978, Rajabizadeh *et al*., 2012, 2016, Mahlow *et al*., 2013). Except for the subgenus *Eoseirenis*, dwarfism occurs in all species of the subgenus *Pseudocyclophis*, as well as in some species of the subgenera *Eirenis* and *Pediohphis*, containing species with <500 mm total (snout to tail) adult size (Mahlow *et al*., 2013). They are known to have a cryptic lifestyle, being found mainly under stones (Terent év and Chernov, 1965; Shwayat *et al*., 2009). Just as for *Eirenis*, some information on the external morphology and taxonomy of the genus *Dolichophis* is available in the literature (Schätti, 1988; Venchi and Sindaco, 2006). These snakes are diurnal surface-dwellers, with an average adult body size of about one meter and a half.

A considerable evolutionary decrease in size from a *Dolichophis*-like ancestor to the miniature *Eirenis* implied an evolutionary modification of the feeding apparatus, and a considerable shift in their diet. *Dolichophis* snakes (maximum size: about 2500 mm, average range: 700–1200 mm) feed on a variety of food items, including small mammals, birds, lizards, and more rarely on bird eggs, arthropods, and even other snakes (Terent év and Chernov, 1965; Göçmen *et al*., 2008; Lelièvre *et al*., 2012; Rajabizadeh, 2018). *Eirenis* (*Pediophis*) *punctatolineatus* (maximum size: 758 mm, average range: 350–550 mm) feeds mainly on lizards (family Lacertidae) and arthropods (of orders Orthoptera, Coleoptera, Hymenoptera, Scolopendromorpha), while *Eirenis* (*Pseudocyclophis*) *persicus* (maximum size: 371 mm, average range: 250–350 mm) feeds nearly exclusively on arthropods (Terent év and Chernov, 1965; Çiçek and Mermer, 2007; Rajabizadeh, 2018). The capacity, especially as a miniature species, to consume prey items bearing a hard exoskeleton suggests the presence of adaptations for feeding on hard prey (Herrel and Holanova, 2008; Schaerlaeken *et al*., 2012). However, the allometric changes in skull shape due to the decrease in body size (see Hanken, 1983) may possibly also predispose these animals to feeding on arthropod prey.

Here, we predict that *Eirenis* miniature subgenera have evolved a different cranial morphology depending on their body size and diet. We hypothesized that (a) cranial morphology in miniature *Eirenis* lineages is different than in *Dolichophis*; and (b) cranial morphology in *Eirenis* lineages and *Dolichophis* reflect a suite of structural adaptations in relation to body size and prey hardness allowing them to take prey items despite smaller body size and/or higher prey hardness. To test this, we provide a detailed structural comparison of the cranial design and the feeding apparatus of *Dolichophis* and *Eirenis* snakes.

2 | MATERIALS AND METHODS

We examined the morphology of the cranial musculoskeletal system in *Dolichophis* and *Eirenis*. Anatomical dissection and three-dimensional reconstructions of the musculoskeletal anatomy of the feeding apparatus are used to visualize and describe the musculoskeletal differences between *Dolichophis* (large bodied, proxy for the ancestral phenotype) and *Eirenis* (two independent lineages of a derived dwarfed phenotype).

2.1 | Specimens

In this study, *Dolichophis schmidti* (Nikolsky, 1909) is considered as a proxy of the ancestral state. *Eirenis* (*Pseudocyclophis*) *persicus*

(Anderson, 1872) and *Eirenis* (*Pediophis*) *punctatolineatus* (Boettger, 1892) represent two subgenera that comprise dwarfed snakes (Figure 2).

Four adult specimens (one *Dolichophis* schmidti, one *Eirenis punctatolineatus*, and two *Eirenis persicus)* were CT-scanned. Moreover, four additional specimens (two *D. schmidti* and two *E. punctatolineatus*) were dissected for osteological examinations (Table 1). Concerning the number of teeth, both data of CT-scanned specimens and literature data (Schätti, 1987; Mahlow *et al*., 2013) were considered. All of the specimens were preserved originally in 96% ethanol for few days (depending on the size of the specimen) and then moved to 75% ethanol for long-term preservation.

2.2 | 3D reconstructions

The micro-CT scans of the heads of three snake specimens were performed at the Centre for X-ray Tomography of the Ghent University (Masschaele *et al*., 2007), using the HECTOR micro-CT scanner (Masschaele *et al*., 2013). Each specimen was μCT-scanned twice, first without any contrast agent, and then after staining with phosphomolybdenic acid (PMA). Staining specimens with PMA allows a detailed discrimination of soft tissue with μCt scanning (Descamps *et al*., 2014). A tube voltage of 130 kV was used. The number of projections and voxel size of the scanned specimens are presented in Table 1.

The raw data were processed and reconstructed using the in-house CT software Octopus (http://www.octopusreconstruction.com; Vlassenbroeck *et al*., 2007) and rendered using Amira V. 5.4.1 (Mercury Systems of Visage Imaging GmbH).

FIGURE 2 *Eirenis punctatolineatus* (a), *E. persicus* (b), and *Dolichophis schmidti* (c) in their natural habitat

2.3 | Osteology and myology

For the descriptions of the bony structures, the terminology used follows that of Romer (1956) and Bullock and Tanner (1966). Muscles were identified following Das and Pramanick (2019).

As an estimate for muscle performance, the average physiological cross-sectional area (hereafter PCSA) of each muscle was defined. The PCSA of a muscle is its cross-sectional area perpendicular to the fibers and is an indicator of its maximum force output (McMahon, 1984; Herrel *et al*., 1997, 1998; Biewener, 2003). We measured it using the relation:

$$\mathrm{PCSA} = \frac{v}{l_f} \quad (1)$$

where v is the muscle volume and l_f is the average muscle fiber length (McMahon, 1984; Biewener, 2003). All PCSA values were multiplied by a maximal force per unit of surface of 40 N/cm^2 (Herrel *et al*., 2007) to obtain an estimate of maximal muscle force. Morphometric data on the muscles were gathered by calculating the fiber lengths and volumes of these muscles using the measurement and surface area modules in AMIRA. As muscle fibers appeared to run throughout the entire length of the muscles, it is possible to measure fiber length as the total muscle length from the origin to insertion (Vincent *et al*., 2009). But, to ensure about the parallel alignment of the muscle fibers throughout the entire muscle, we made slices across the length of each jaw muscle (using oblique slice modules in AMIRA) and followed at least three muscle fibers from the origin to insertion and measured the average length of these fibers.

We measured the volume (in mm^3) and length (in mm) of the following cranial muscles of which it has been shown that they are important during snake feeding (Cundall and Gans, 1979; Cundall, 1983; Kardong, 1986; Kardong *et al*., 1986; Schwenk, 2000; Moon *et al*., 2019): levator anguli oris (LAO), adductor mandibulae externus medialis profundus (AEMP), adductor mandibulae externus superficialis (AES), pseudotemporalis (Psu), depressor mandibulae (DM), pterygomandibularis (PTM), pterygomandibularis accessories (PTM accessories), protractor pterygoidei (PP), levator pterygoidei (LP), and protractor quadrati (PQ).

2.4 | Gape

To compute gape, cross-sectional area of the posterior oral cavity and anterior esophagus appears to be critical (Cundall *et al*., 2014). The lengths of the lower jaw and suspensory elements, and the width of the head, have been hypothesized to be particularly important because they could affect the maximum size of the mouth opening (Miller and Mushinsky, 1990; Cundall and Greene, 2000;

TABLE 1 List of the examined specimens as well as the number of projections and voxel size of the scanned specimens

Species	SVL (mm)	Dissected	CT-scanned	Number of projections		Voxel size (μm)	
				Regular	PMA-stained	Regular	PMA-stained
Dolichophis schmidti	750		√	1762	862	19.863	0.055
Dolichophis schmidti	600	√		–			
Dolichophis schmidti	700	√		–			
Eirenis punctatolineatus	408		√	1781	890	11.261	0.011
Eirenis punctatolineatus	399	√		–			
Eirenis punctatolineatus	368	√		–			
Eirenis persicus	233		√	1802	1632	6.2	0.008
Eirenis persicus	277		√	1683	–	9.454	–

King, 2002; Hampton and Moon, 2013). These morphological indicators of gape did not prove to be the best indicators of actual gape, since the gape values they produced differed significantly from the empirically determined gapes in alive specimens (Hampton and Moon, 2013) probably because the properties of soft tissues may be critical in determining maximum gape areas or angles (Close and Cundall, 2014; Close *et al*., 2014; Cundall *et al*., 2014). But, cranial measurements provide a good estimate of actual gape in preserved specimens that is comparable among the taxa and lineages. Hence, to calculate a gape index, we followed King (2002) and Miller and Mushinsky (1990) formula:

$$\text{Gape index} = \frac{\pi \times (\text{jaw length}) \times (\text{jaw width})}{4}. \quad (2)$$

Jaw length was measured from the posterior end of the retroarticular process to the tip of the dentary. Following King (2002) and Miller and Mushinsky (1990), jaw width was measured in live specimens, as the transverse distance at the jaw articulation, when applying pressure on the posterior portion of the head to spread the quadrates and mandibles laterally. The computed gape index represents the cross-sectional area as the area of an ellipse with major and minor axes equal to jaw length and jaw width, respectively (see King, 2002). This index is based on the expected contributions of the head width and length to swallowing ability (Miller and Mushinsky, 1990; King, 2002). Since an insufficient number of live *Eirenis* specimens were available, we used the preserved museum samples and measured the head width as a proxy of jaw width. Hence, we computed a proxy of gape index in seven specimens of *Dolichophis schmidti* and 245 specimens belonging to 14 species (of four subgenera) of the genus *Eirenis*, including subgenus *Pseudocyclophus* (*E. occidentalis*, *E. persicus*, *E. nigrofasciatus*, *E. walteri*, *E. angusticeps*); subgenus *Eirenis* (*E. aurolineatus*, *E. modestus*); subgenus *Eoseirenis* (*E. decemlineatus*); and subgenus *Pediophis* (*E. barani*, *E. coronelloides*, *E. eiselti*, *E. levantinus*, *E. rothi*, *E. punctatolineatus*) (for details of the examined museum specimens see Table S1). Length measurements used to calculate gape index were carried out using calipers to the nearest 0.1 mm. Since the accuracy of morphological measurements of snakes (especially head width and SVL) has been questioned recently (Cundall *et al*., 2016), to reduce the measurement errors, only one person (A. Avci) performed all the measurement, solely on preserved specimens. For the scaling analysis of the gape index, reduced major axis (RMA) regression of the log-transformed variables (*y*-axis) against the log-transformed head length and log-transformed snout–vent length (*x*-axis) was computed, which is more robust in preventing spurious correlations which arise from the use of ratios in regression analysis (Rayner, 1985). With these RMA regression results, we tested whether the slope of gape index remained the same or changed with a decrease in body and head size in 14 *Dolichophis*–*Eirenis* lineages, including *D. schmidti*, and all *Eirenis* species. We then compared the allometry of the slopes with those predicted values under a model of geometric similarity (McMahon, 1984). The significance of the difference between the observed slopes and those predicted under a geometric similarity model in gape index was checked by testing for correlation between residual and fitted values, following Taskinen and Warton (2013). Allometric analyses were performed using lmodel2 package (Legendre, 2018) and smatr package (Warton *et al*., 2012).

To visualize the allometry of gape size in a phylogenetic context, we used a phylomorphospace approach. In this analysis, the cladogram is a pruned tree, modified after Nagy *et al*. (2003), comprising *Dolichophis schmidti* and 14 *Eirenis* species (as mentioned above). The phylogenetic tree was projected into a biplot of log-transformed average total length versus average gape size of the examined specimens. The analysis was performed using the phylomorphospace function in phytools package v. 0.6–60 (Revell *et al*., 2012). All analyses were performed in the R environment (R Core Team, 2014).

3 | RESULTS

3.1 | Descriptive osteological comparison

The skull of *Dolichophis schmidti* is long and elliptic, well-ossified, and composed of robust and thick bones. On the tip of the snout, the single, pyramid-shaped premaxilla is wedged between the nasals (Figures 3–5).

The neurocranium is long, composed of thick, compactly ossified bones that are attached to each other by completely fused sutures to form a complete enclosure for the brain.

The palatomaxillary arches are composed of thick bony elements. The left and right palatines are long and narrow bones, each of them articulating with the prefrontal process of the maxilla laterally and with the pterygoid posteriorly. Each palatine bears a longitudinal row of nine posteriorly curved teeth of similar size. The pterygoids are a pair of long, flattened, bar-like, slightly bended elements, extending from the posterior end of the palatines to the posterior mandibles. Each of the pterygoids bears a row of 14–15 teeth (add to the literatures data: 14–19) on its anterior half. The tooth rows end at the level of basisphenoid and exoccipital suture, where the pterygoid bends toward the posterior mandible. The ectopterygoids are flat bones, anteriorly bifurcated, and posteriorly notched, connecting the maxillae to the pterygoids. The left and right maxillae are curved bones, posteriorly somewhat broadened, connected to the flattened ventral surface of the ectopterygoid, medially articulating with the ventral surface of the prefrontal via a mesial process. Each maxilla bears sockets for 11 (11–13) anterior teeth of similar size after a space (nearly one tooth length) are followed by two bigger teeth (about 1.5 times longer than the anterior teeth).

The left and right mandibles are long, dorsally concave, connected to each other anteriorly by an elastic ligament. Each mandible unit is composed of two major bones, the compound bone and the dentary. The dentary forms approximately the anterior half of the lower jaw and bears 12 (12–17) teeth that decrease in size toward the posterior dentary.

The skull bones in *Eirenis punctatolineatus* are generally similar to those of *Dolichophis schmidti*, but they are less robust and thick,

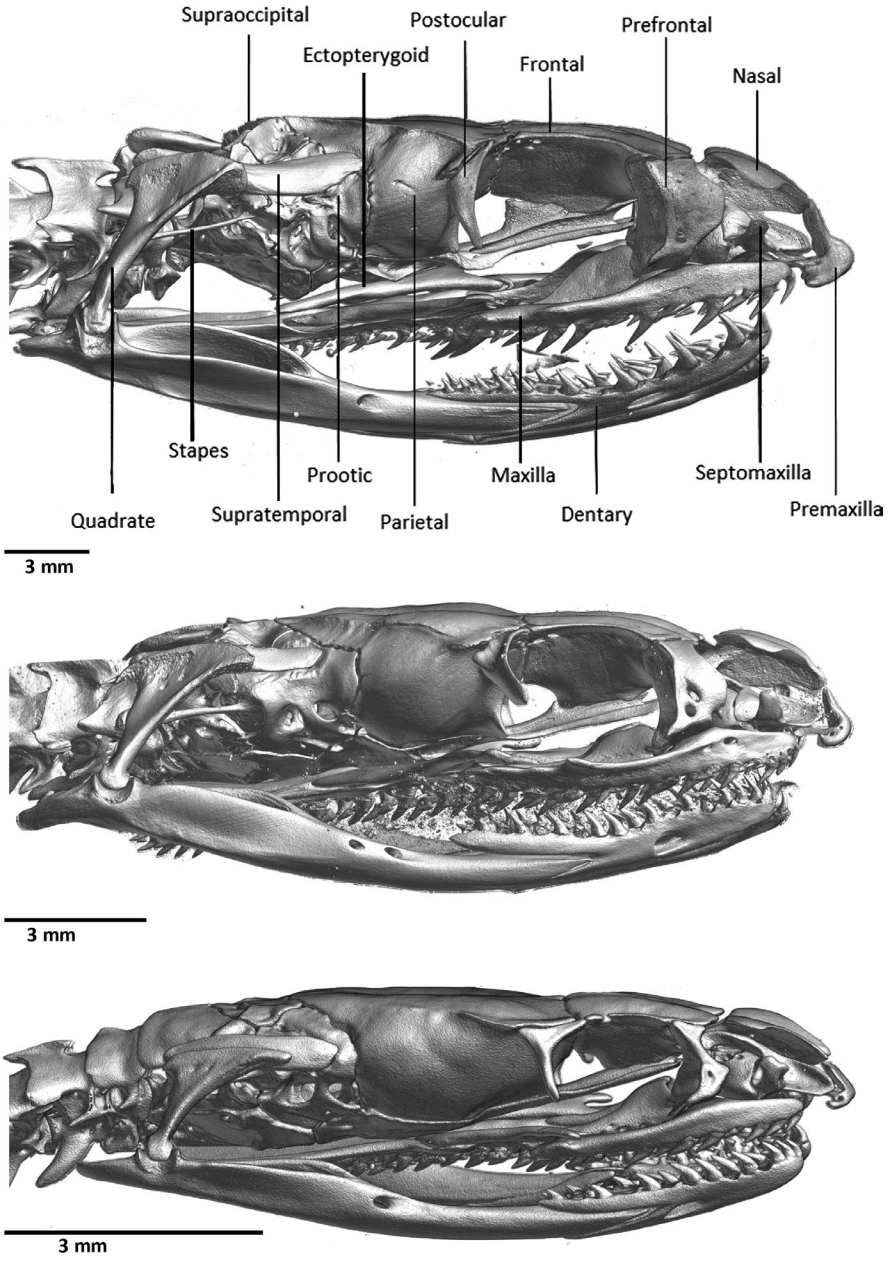

FIGURE 3 Lateral views of the skulls of *Dolichophis schmidti* (top), *Eirenis punctatolineatus* (middle), and *Eirenis persicus* (bottom)

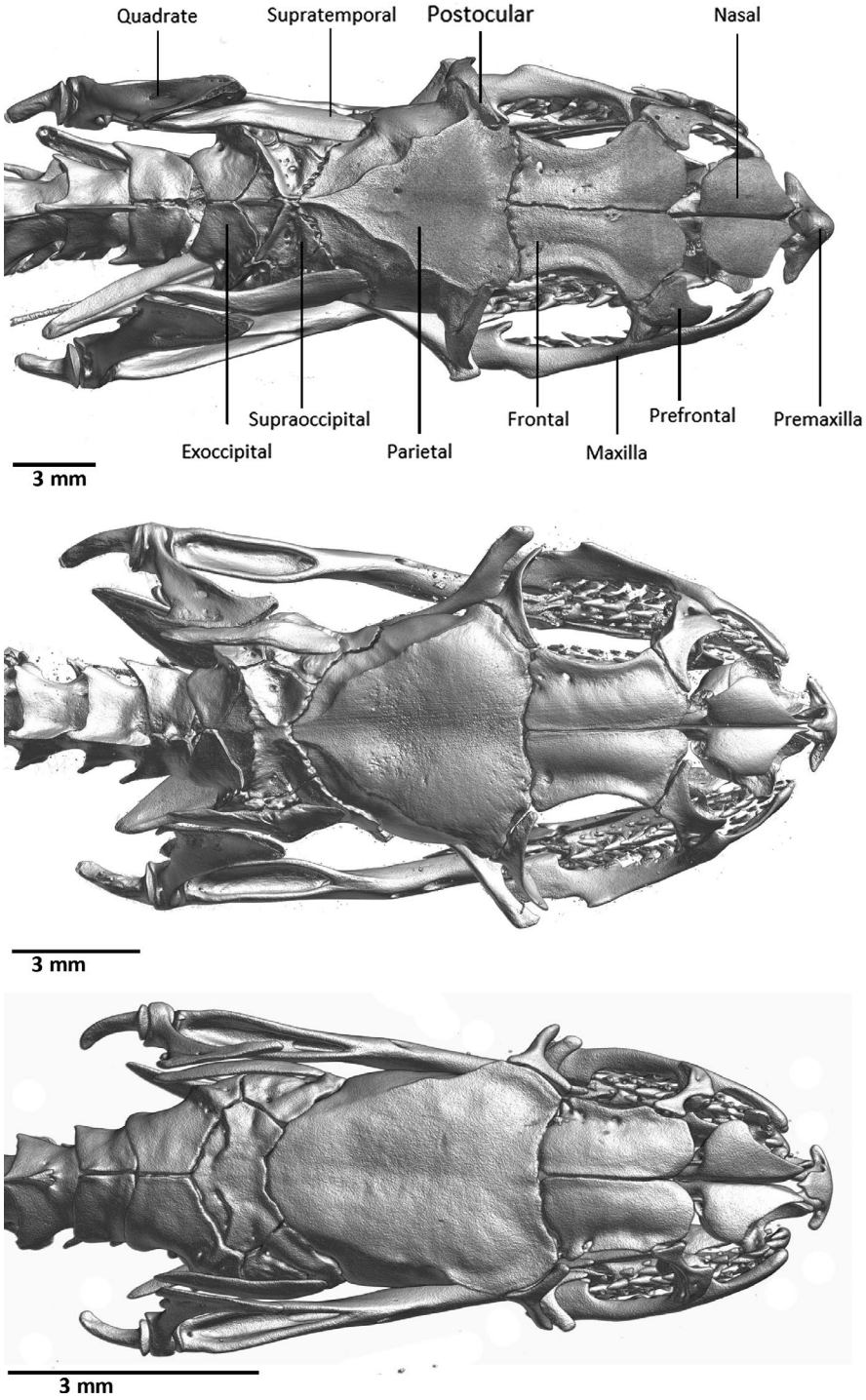

FIGURE 4 Dorsal views of the skulls of *Dolichophis schmidti* (top), *Eirenis punctatolineatus* (middle), and *Eirenis persicus* (bottom)

having less denticulate sutures and looser articulation with one another. Compared to *D. schmidti*, in *E. punctatolineatus* the neurocranium is relatively wider, bearing a less elaborated V-shaped pair of crests on the parietal bones. The premaxilla is smaller, less projected anteriorly, and wedged between the tips of nasals dorsally. Maxillary teeth are homogenous, and there are 19 (17–21) teeth of similar size on each maxilla. Each palatine bears a row of 10 (10–12) teeth of the same size. Each pterygoid bears a row of 18–19 (16–22) similarly sized teeth extending nearly across the length of the bone. The pterygoids project beyond the brain case to the level of the first (atlas) and second (axis) cervical vertebrae. The dentary bears sockets for 20 (17–22) teeth that decrease in size toward the posterior side.

Compared to *E. punctatolineatus* and *D. schmidti*, the skull in *Eirenis persicus* is more round and the skull bones are generally thinner, less robust, and attached to each other by smooth and open sutures. The neurocranium is wider, oval-shaped, bearing no elaborated V-shaped pair of crests on parietal bones, and the braincase is larger. The maxillary teeth are homogenous, and there are 13–16 (13–17) similarly sized teeth on each maxilla. The premaxilla is smaller, not projected anteriorly, and wedged between the tips of nasals dorsally. Each

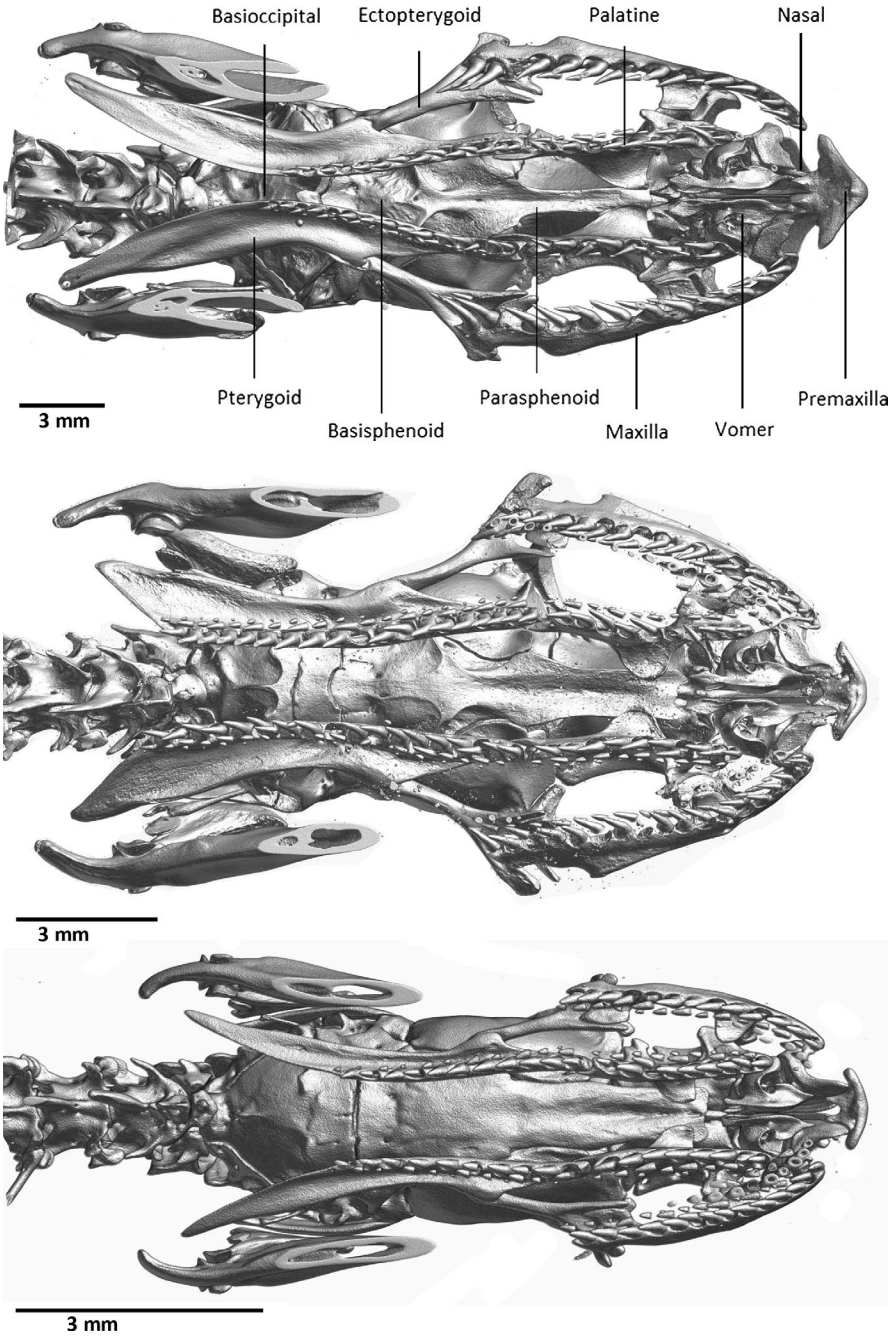

FIGURE 5 Ventral views of the skulls of *Dolichophis schmidti* (top), *Eirenis punctatolineatus* (middle), and *Eirenis persicus* (bottom)

palatine bears a row of 8–11 similarly sized teeth. Each pterygoid bears a row of 10–16 (10–17) teeth of similar size on its anterior two thirds. Each dentary bears sockets for 14–18 teeth that decrease in size posteriorly. Teeth in *E. persicus* are generally conically shaped and blunt compared with the more elongated and sharper teeth in *E. punctatolineatus* and *D. schmidti*.

3.2 | Qualitative myology

The levator anguli oris, adductor mandibulae externus medialis profundus, adductor mandibulae externus superficialis, and pseudotemporalis are responsible for closing the lower jaw (Figure 6). In *Dolichophis schmidti*, of three jaw adductor muscles, the levator anguli oris is the most anterior and superficial. It is a triangularly shaped muscle, originating from the lateral wall of the parietal bone (just in front of the supratemporal) and the upper half of the postorbital, and inserts onto a point near the middle of the mandible on the lateral edge of the anterior portion of the compound bone. The adductor mandibulae externus medialis profundus is largely covered by the levator anguli oris and the adductor mandibulae externus superficialis. It is a triangular muscle, originating primarily from the sagittal crest of the parietal bone and inserting onto the dorsomedial and dorsolateral surfaces in front of the dorsal groove of the compound bone. The adductor mandibulae externus superficialis is the largest adductor muscle, covered anteriorly by the levator anguli oris. It is a triangular

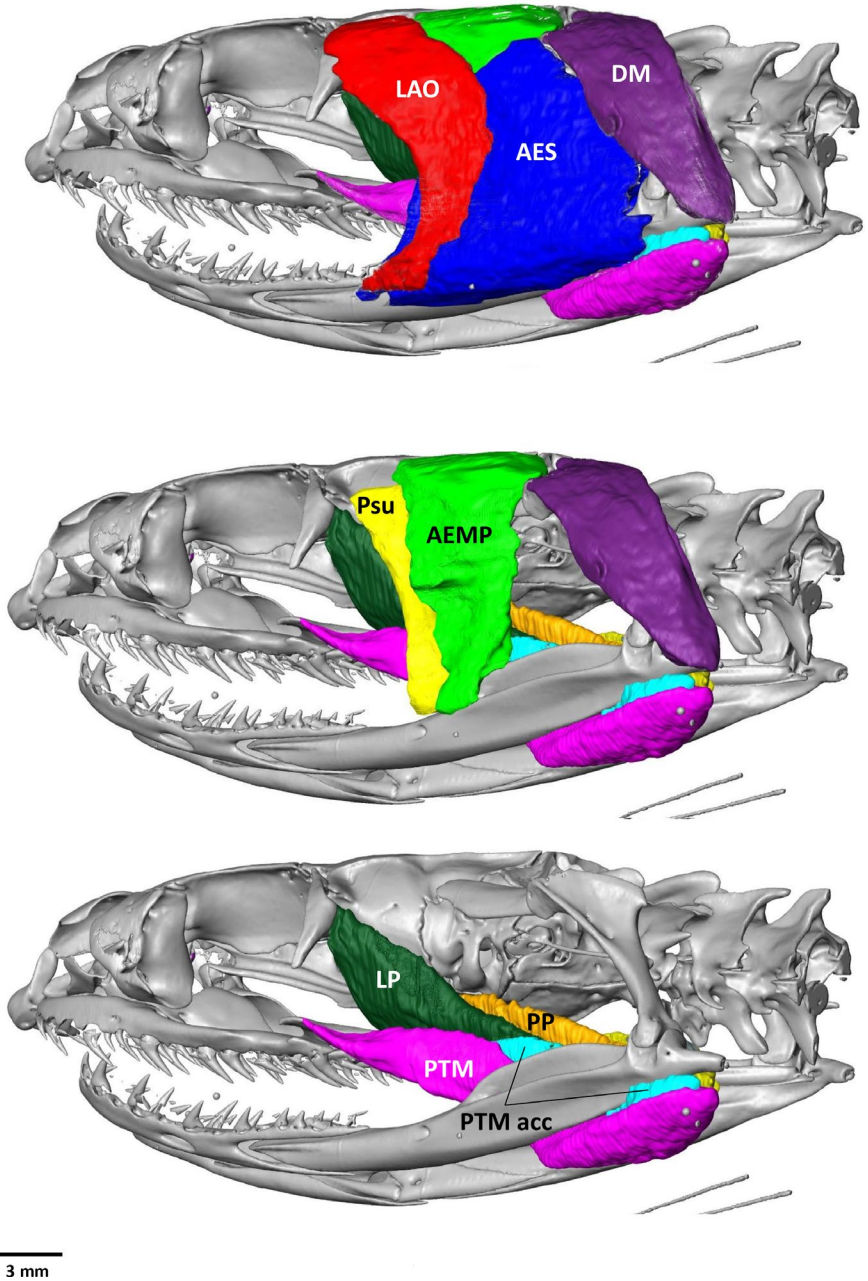

FIGURE 6 Cranial muscles in *Dolichophis schmidti*. For abbreviations, see materials and methods, subtitle osteology, and myology

muscle that originates on the anterolateral edge of the quadrate bone and inserts broadly along the lateral surface of the compound bone between the quadrato-mandibular joint and the insertion point of the levator anguli oris. The pseudotemporalis is a long and narrow muscle, mainly covered by the adductor mandibulae externus medialis profundus, that originates from the lateral wall of the parietal bone (just below the origin of the adductor mandibulae externus medialis profundus) and inserts between the insertion points of levator anguli oris and adductor mandibulae externus medialis profundus.

The musculus depressor mandibulae originates from the anterior lateral and medial, proximal end of the quadrate and inserts onto the dorsomedial aspect of the retroarticular process. The pterygomandibularis is an elongated, pyriform muscle, originating at the anterodorsal edge of the ectopterygoid (ectopterygoid–maxilla articulation), extending between the mandible and the pterygoid, and inserting on the lateral, posterior, and ventral surfaces of the postarticular process of the mandible. This muscle protracts the mandible. The pterygomandibularis accessories is a short muscle, originating along the dorsolateral surface of the pterygoid bone and inserting on the medial surface of the mandible, close to but below the quadrato-mandibular articulation. The pterygomandibularis accessories is a broad muscle originating on the ventral and lateral sides of the basisphenoid; it extends across the posterior pterygoid bone and inserts on the dorsomedial surface of the pterygoid. The musculus levator pterygoidei originates from the postorbital–parietal articulation and inserts broadly on the pterygoid, along its dorsal surface. The muscle protractor quadrati is a thin and flat muscle, originating from the ventral surface of the basioccipital and inserting on the distal end of the quadrate and the associated region of the compound bone.

In the *E. punctatolineatus* and *Eirenis persicus*, the levator anguli oris and adductor mandibulae externus superficialis are more or less similar to those described for *D. schmidti*, but the adductor mandibulae externus medialis profundus has a broader insertion along the anterior dorsal groove of the compound bone. The pseudotemporalis in *Eirenis punctatolineatus* and *Eirenis persicus* is more rectangular in shape than in *D. schmidti*. The rest of the cranial muscles are more or less similar to those of the *D. schmidti*.

3.3 | Quantitative myology comparison

Muscle volume, muscle fiber length, and physiological cross-sectional area (PCSA) of the 10 cranial muscles that are responsible for feeding in *Dolichophis schmidti*, *Eirenis punctatolineatus*, and *Eirenis persicus* are presented in Table 2. The maximal muscle force generated by the cranial muscles, scaled to the respected head length of each species, is presented in Figure 7.

3.4 | Scaling of head dimensions

3.4.1 | Scaling to snout-vent length

In scaling of head characters to the snout–vent length, the head width and the gape index exhibited a significant negative allometry compared with the slopes predicted by a model of geometric similarity in the transition from *Dolichophis schmidti* to the *Eirenis* and *Pediophis* subgenera, but these characters decreased nearly isometrically in *D. schmidti* to *Eoseirenis* and *Pseudocyclophis* subgenera (except in *E. occidentalis*) (Tables 3 and 4). In scaling to the snout–vent length, the head length exhibited significant negative allometry compared with the slopes predicted by a model of geometric similarity in the transition from *Dolichophis schmidti* to *Eirenis*, *Eoseirenis*, and *Pediophis* subgenera, but these characters decreased nearly isometrically in *Dolichophis schmidti–Pseudocyclophis* subgenus. In conclusion, *Eirenis* snakes of the subgenera *Eirenis* and *Pediophis* have relatively larger head (both longer and wider), and those of the subgenus *Eoseirenis* have a relatively longer head for their body size, compared with *D. schmidti*. Also, all *Eirenis* subgenera except *Pseudocyclophis* have a relatively larger gape index for their body size, compared with *D. schmidti*, but this characters decreased nearly isometrically in *Dolichophis schmidti* to *Pseudocyclophis* subgenus (Tables 3 and 4) (Figure 8).

3.4.2 | Scaling to head length

When scaling head dimensions to head length, gape index exhibited a significant negative allometry in the *Pseudocyclophis* subgenus ($p = .66$ in *E. walteri*) (Table 3), but decreased nearly isometrically in the *Eirenis*, *Eoseirenis*, and *Pediophis* subgenera (except for *E. modestus* and *E. coronelloides*). Therefore, *Eirenis* snakes of the subgenus *Pseudocyclophis* have a relatively larger gape index for their head size, compared with *D. schmidti*.

4 | DISCUSSION

Our results indicate clear osteological and myological differences between the dwarfed *Eirenis* species and *Dolichophis*. Variation in the cranial morphology could be explained partly as a result of mechanical (physical) interactions among the skeletal, nervous, and sensory

TABLE 2 Muscle volume, muscle fiber length, and physiological cross-sectional area (PCSA) of feeding muscles in *Dolichophis schmidti*, *Eirenis punctatolineatus*, and *Eirenis persicus*

	Muscle volume (cm^3)			Muscle fiber length (cm)			PCSA (cm^2)		
Muscle	*D. schmidti*	*E. punctat.*	*E. persicus*	*D. schmidti*	*E. punctat.*	*E. persicus*	*D. schmidti*	*E. punctat.*	*E. persicus*
Levator anguli oris	0.069224	0.007826	0.000657	1.6048	0.6717	0.2694	0.043	0.012	0.002
Adductor mandibulae externus medialis profundus	0.102108	0.006625	0.000676	1.1613	0.3373	0.1365	0.088	0.02	0.005
Adductor mandibulae externus superficialis	0.302775	0.017456	0.001874	1.2285	0.3946	0.2196	0.246	0.044	0.009
Pseudotemporalis	0.014611	0.001947	0.000148	1.1146	0.3489	0.1571	0.013	0.006	0.001
Depressor mandibulae	0.090764	0.006013	0.000578	1.6105	0.5729	0.2172	0.056	0.01	0.003
Pterygomandibularis	0.141221	0.01213	0.001469	2.442	1.0255	0.4758	0.058	0.012	0.003
Pterygomandibularis accessories	0.0393	0.002869	0.000466	1.5362	0.6352	0.2849	0.026	0.005	0.002
Protractor pterygoidei	0.06665	0.004799	0.000598	1.6927	0.6801	0.2967	0.039	0.007	0.002
Levator pterygoidei	0.045953	0.00369	0.000404	1.1687	0.5464	0.2885	0.039	0.007	0.001
Protractor quadrati	0.035044	0.002227	0.000289	1.0818	0.34	0.1616	0.032	0.007	0.002

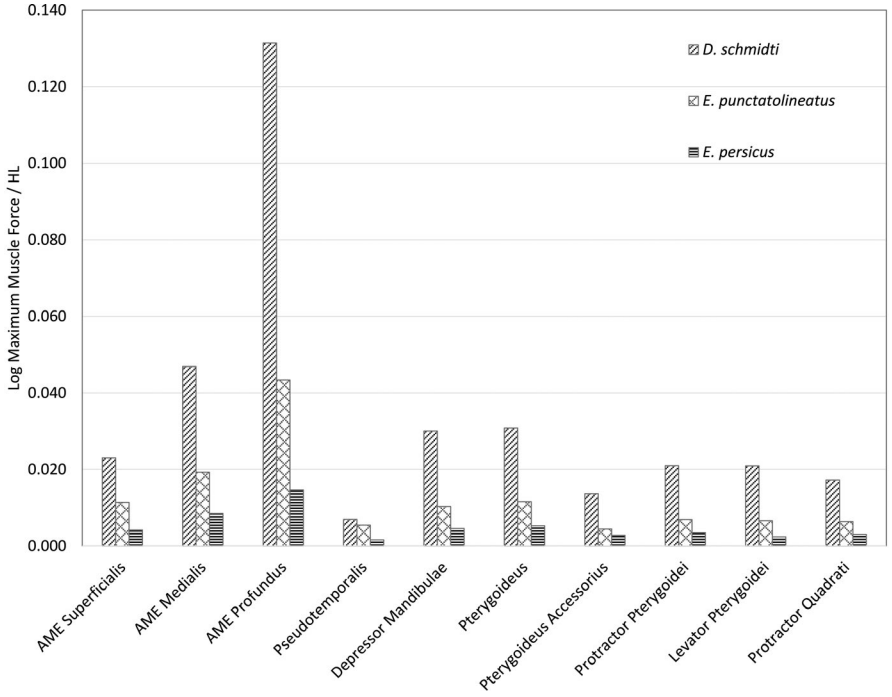

FIGURE 7 Maximal muscle force (N) of feeding muscles, scaled to the SVL (cm), in *Dolichophis schmidti*, *Eirenis punctatolineatus*, and *Eirenis persicus*

TABLE 3 Results of reduced major axis regression of $\log_{10}$-transformed gape index against $\log_{10}$-transformed snout–vent length and $\log_{10}$-transformed head length

	Gape index (cm^2)/SVL (cm)					Gape index (cm^2)/HL (cm)				
Subgenus	**Slope**	**CI 97.5%**	**Y intercept**	R^2	*p*	**Slope**	**CI 97.5%**	**Y intercept**	R^2	*p*
Pseudocyclophis										
D. schmidti–E. occidentalis	2.107	2.287	−3.636	.980	.195	**1.781**	1.855	−0.049	.995	.000
D. schmidti–E. persicus	1.939	2.151	−3.137	.970	.530	**1.852**	1.934	−0.162	.995	.002
D. schmidti–E. nigrofasciatus	2.069	2.286	−3.521	.977	.473	**1.916**	2.001	−0.257	.996	.053
D. schmidti–E. walteri	2.136	2.462	−3.723	.959	.327	1.908	2.007	−0.244	.995	.066
D. schmidti–E. angusticeps	2.049	2.270	−3.464	.976	.612	**1.914**	2.001	−0.252	.996	.052
Eirenis										
D. schmidti–E. aurolineatus	**1.313**	1.521	−1.273	.950	.000	2.082	2.281	−0.506	.981	.358
D. schmidti–E. modestus	**1.410**	1.576	−1.568	.910	.000	**1.844**	1.961	−0.147	.973	.011
Eoseirenis										
D. schmidti–E. decemlineatus	1.735	2.043	−2.533	.939	.082	2.071	2.228	−0.490	.988	.313
Pediophis										
D. schmidti–E. barani	**1.406**	1.515	−1.541	.963	.000	1.937	2.018	−0.293	.989	.119
D. schmidti–E. coronelloides	**1.387**	1.513	−1.497	.979	.000	**1.826**	1.905	−0.120	.995	.000
D. schmidti–E. eiselti	**1.503**	1.588	−1.831	.939	.000	1.982	2.056	−0.357	.973	.627
D. schmidti–E. levantinus	**1.348**	1.475	−1.373	.967	.000	2.037	2.170	−0.441	.984	.549
D. schmidti–E. rothi	**1.594**	1.767	−2.106	.959	.000	1.992	2.110	−0.374	.987	.886
D. schmidti–E. punctatolineatus	**1.203**	1.313	−0.927	.908	.000	1.928	2.063	−0.255	.946	.283

Note: Significant values are in bold.

components during head development at reduced size (Hanken, 1983). Maintenance of the skull functions becomes more difficult as external dimensions are constrained, so different structures will respond differently to changes in scale in order to maintain functional efficiency (Hanken, 1983).

4.1 | Brain size variation

The occurrence of a larger and more oval-shaped braincase in *Eirenis* snakes indicates that during the evolutionary transformation across the *Dolichophis–Eirenis* lineages, brain size likely does

TABLE 4 Results of reduced major axis regression of $\log_{10}$-transformed head length and $\log_{10}$-transformed head width against $\log_{10}$-transformed snout–vent length

	HL/SVL					HW/SVL				
Subgenus	**Slope**	**CI 97.5%**	***Y* intercept**	R^2	***p***	**Slope**	**CI 97.5%**	***Y* intercept**	R^2	***p***
Pseudocyclophis										
D. schmidti–E. occidentalis	**1.185**	1.288	−2.02	.978	.001	0.928	1.033	−1.527	.966	.159
D. schmidti–E. persicus	1.048	1.165	−1.608	.97	.357	0.896	1.015	−1.436	.958	.079
D. schmidti–E. nigrofasciatus	1.081	1.203	−1.707	.975	.136	1.000	1.123	−1.744	.970	.999
D. schmidti–E. walteri	1.122	1.299	−1.831	.96	.105	1.022	1.207	−1.810	.948	.773
D. schmidti–E. angusticeps	1.072	1.196	−1.681	.974	.189	0.989	1.113	−1.710	.969	.837
Eirenis										
D. schmidti–E. aurolineatus	**0.621**	0.738	−0.342	.933	.000	**0.684**	0.812	−0.805	.935	.000
D. schmidti–E. modestus	**0.756**	0.844	−0.747	.919	.000	**0.644**	0.754	−0.688	.839	.000
Eoseirenis										
D. schmidti–E. decemlineatus	**0.833**	0.98	−0.974	.944	.03	0.901	1.103	−1.450	.914	.281
Pediophis										
D. schmidti–E. barani	**0.72**	0.792	−0.629	.948	.000	**0.689**	0.748	−0.815	.956	.000
D. schmidti–E. coronelloides	**0.758**	0.829	−0.748	.979	.000	**0.629**	0.707	−0.641	.966	.000
D. schmidti–E. eiselti	**0.749**	0.808	−0.722	.918	.000	**0.755**	0.809	−1.008	.911	.000
D. schmidti–E. levantinus	**0.656**	0.734	−0.442	.956	.000	**0.687**	0.776	−0.811	.948	.000
D. schmidti–E. rothi	**0.795**	0.901	−0.857	.946	.001	**0.799**	0.904	−1.145	.947	.001
D. schmidti–E. punctatolineatus	**0.613**	0.674	−0.322	.927	.000	**0.584**	0.706	−0.487	.788	.000

Note: Significant values are in bold.

not scaled isometrically with body size. The size of the neurocranium in the *Dolichophis–Eirenis* lineage indicates that miniature *Eirenis* snakes likely have a relatively larger brain size than *Dolichophis* snakes.

Many examples of negative allometry of the brain size relative to body size have been reported in the dwarfed vertebrates (Roth *et al*., 1995; Yeh, 2002; Weston and Lister, 2009). Bauchot (1978) argues that generally negative allometry of the brain size relative to body size is typical of vertebrates more generally.

Brain size and body size present an excellent example of two highly positively correlated traits across various taxonomic levels (Striedter, 2005). Various explanations have been proposed regarding the negative allometry of brain size relative to body size. Roth *et al*. (1995), in studying miniaturization in plethodontid salamanders, observed that although the brain in *Thorius* loses cells during miniaturization, there is a minimal threshold for the number of brain neuronal cells to maintain proper function. So, in closely related taxa, the larger relative brain size in the miniature descendants may refer to the structural and functional consequences of dwarfing. Negative allometric decrease in brain size through miniaturization may reflect a size threshold for the brain to maintain all neuronal activities required (Hanken and Wake, 1993), as has been suggested for different amphibians and reptiles (e.g., Roth *et al*., 1995; Striedter, 2005). Larger relative brain size is an advantage for dwarfed evolved descendant (genus *Eirenis*), since it is generally associated with increased cognitive abilities. Recent comparative analyses have shown positive associations between relative brain size and survival (Sol *et al*., 2008) and innovative behavior (Lefebvre *et al*., 2004).

4.2 | Cranial variation

Negative allometry of the gape index relative to body size, observed across the transition from the *Dolichophis* to *Pediophis* and *Eirenis* subgenera, suggests that during the miniaturization in these subgenera, they achieved a greater gape index compared with the ancestral condition, while an isometric decrease in gape index is observed during the transition from the *Dolichophis* to *Eoseirenis* and *Pseudocyclophis* subgenera. Considering the large body size of *Eirenis* (*Eoseirenis*) *decemlineata* (maximum body size 900 mm) and the fact that miniaturization did not occur in this lineage, the isometric decrease in the gape index in this lineage is not surprising.

The difference in gape index in the rest of the subgenera could be explained based on differences in prey type. Hence, while *Eirenis* and *Pediophis* feed on arthropods and lizards (Terent év and Chernov, 1965; Çıçek and Mermer, 2007; Shwayat *et al*., 2009), *Pseudocyclophis* snakes feed on arthropods exclusively (Terent év and Chernov, 1965). Many studies showed a correlation between gape index and the prey type eaten in snakes (King, 2002; Vincent *et al*., 2007; Vincent *et al*., 2009; Brecko *et al*., 2011; Hampton, 2011; Hampton, 2014). In a gape-limited predator, maximum gape size primarily determines the size, shape, and the type of the prey that can

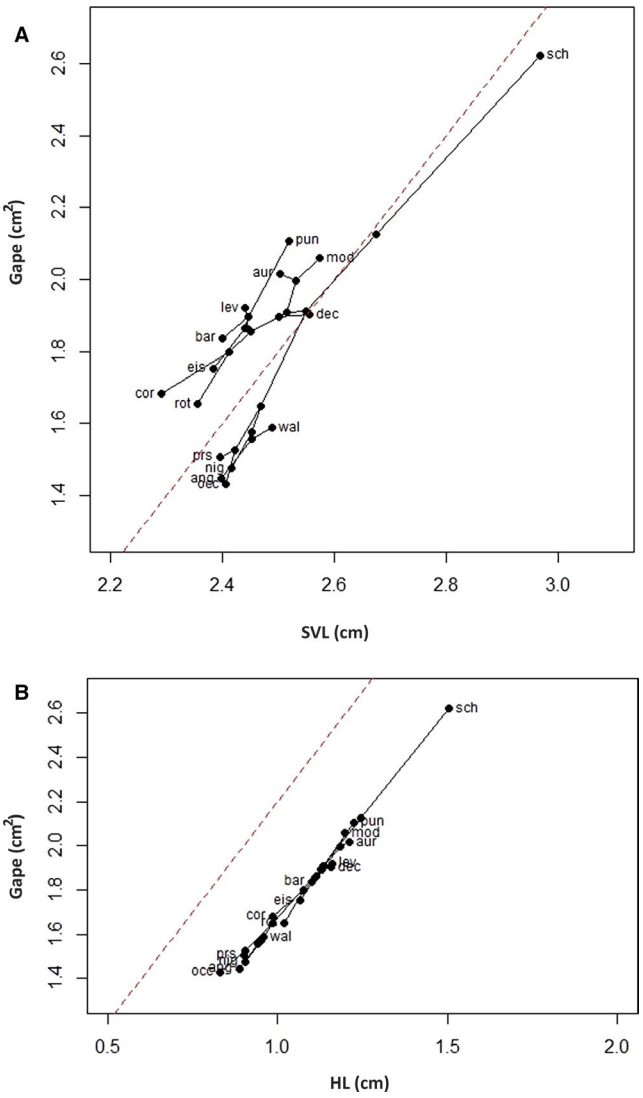

FIGURE 8 Phylomorphospace showing the relationships between the $\log_{10}$-transformed gape index against $\log_{10}$-transformed snout–vent length (a) and $\log_{10}$-transformed gape index against the $\log_{10}$-transformed head length (b) among *Dolichophis schmidti* (sch) and 14 species of the genus *Eirenis* (subgenus *Pseudocyclophus* (*E. occidentalis* (occ), *E. persicus* (prs), *E. nigrofasciatus* (nig), *E. walteri* (wal), *E. angusticeps* (ang)); subgenus *Eirenis* (*E. aurolineatus* (aur), *E. modestus* (mod)); subgenus *Eoseirenis* (*E. decemlineatus* (dec)); and subgenus *Pediophis* (*E. barani* (bar), *E. coronelloides* (cor), *E. eiselti* (eis), *E. levantinus* (lev), *E. rothi* (rot), *E. punctatolineatus* (pun)). The dash line indicates the slope of the log–log regression of area (*y*) against length (*x*) under isometric scaling (area = 2)

be successfully ingested (Cundall and Greene, 2000). A larger gape should increase the variety of prey shapes and sizes that can be consumed and increase the energy acquisition (Forsman, 1996).

Hence, the increased gape size relative to the body size in *Eirenis* and *Pediophis* is likely an adaptation that enables them to feed on a variety of food items (e.g., arthropods and lizards) even at small size.

When exploring the gape index relative to head length, negative allometry only observed in *Pseudocyclophis*, suggesting that during miniaturization among *Eirenis* subgenera, only the subgenus *Pseudocyclophis* achieved a relatively greater gape size relative to its head size. Increased gape size relative to the head length could aid in the intraoral transport (Vincent *et al*., 2006). Hence, although the *Pseudocyclophis* lineage does not eat large and diverse prey, but their increased intraoral transport may enable them to swallow more massive, yet elongate prey like centipedes (personal observation) without the necessity for exceptionally large gape relative to body size.

TABLE 5 Descriptive comparison of gape index and PCSA of jaw muscles between *Dolichophis schmidti*, *Eirenis punctatolineatus*, and *Eirenis persicus*

	D. schmidti/ *E. punctatolineatus*	*D. schmidti*/ *E. persicus*
Gape index	3.2	16.7
Levator anguli oris	2.0	5.5
Adductor mandibulae externus medialis profundus	2.4	5.5
Adductor mandibulae externus superficialis	3.0	9.0
Pseudotemporalis	1.3	4.3
Depressor mandibulae	2.9	6.6
Pterygomandibularis	2.7	5.8
Pterygomandibularis accessories	3.1	4.9
Protractor pterygoidei	3.0	6.1
Levator anguli oris	3.2	8.7
Adductor mandibulae externus medialis profundus	2.7	5.6

Note: The numbers indicate how the gape index and PCSA of jaw muscles of *D. schmidti* are larger than those traits in *E. punctatolineatus* or *E. persicus*. Both gape index and PCSA have the same scale, mm^2.

4.3 | Jaw muscle variations

Data on the PCSA of dwarfed lineages are not available for other reptiles. A qualitative comparison of the available PCSA data of jaw muscles (Table 5) reveals that the PCSA data of *D. schmidti* are about 2–3.2 times larger than that in *E. punctatolineatus* (except for the pseudotemporalis). Moreover, the PCSA data of *D. schmidti* are around 4.9–9 times larger than that in *E. persicus*. The similarity in PCSA between *E. punctatolineatus* and *D. schmidti* could be explained by their similarity in diet.

Superimposing the PCSA data of the species studied here with the data for an ontogenetic series of a colubrid snake, *Nerodia fasciata* (Vincent *et al*., 2007), we assessed the general consequence of miniaturization (Figure 9). Interestingly, the PCSA data for the snakes in our study do not follow the ontogenetic pattern described for *N. fasciata*. The slopes of jaw muscles' PCSA against head length exhibit a very strong positive allometry in banded water snakes (Vincent *et al*., 2007). This contrasts data found in our own work for the snakes of the *Dolichophis–Eirenis*

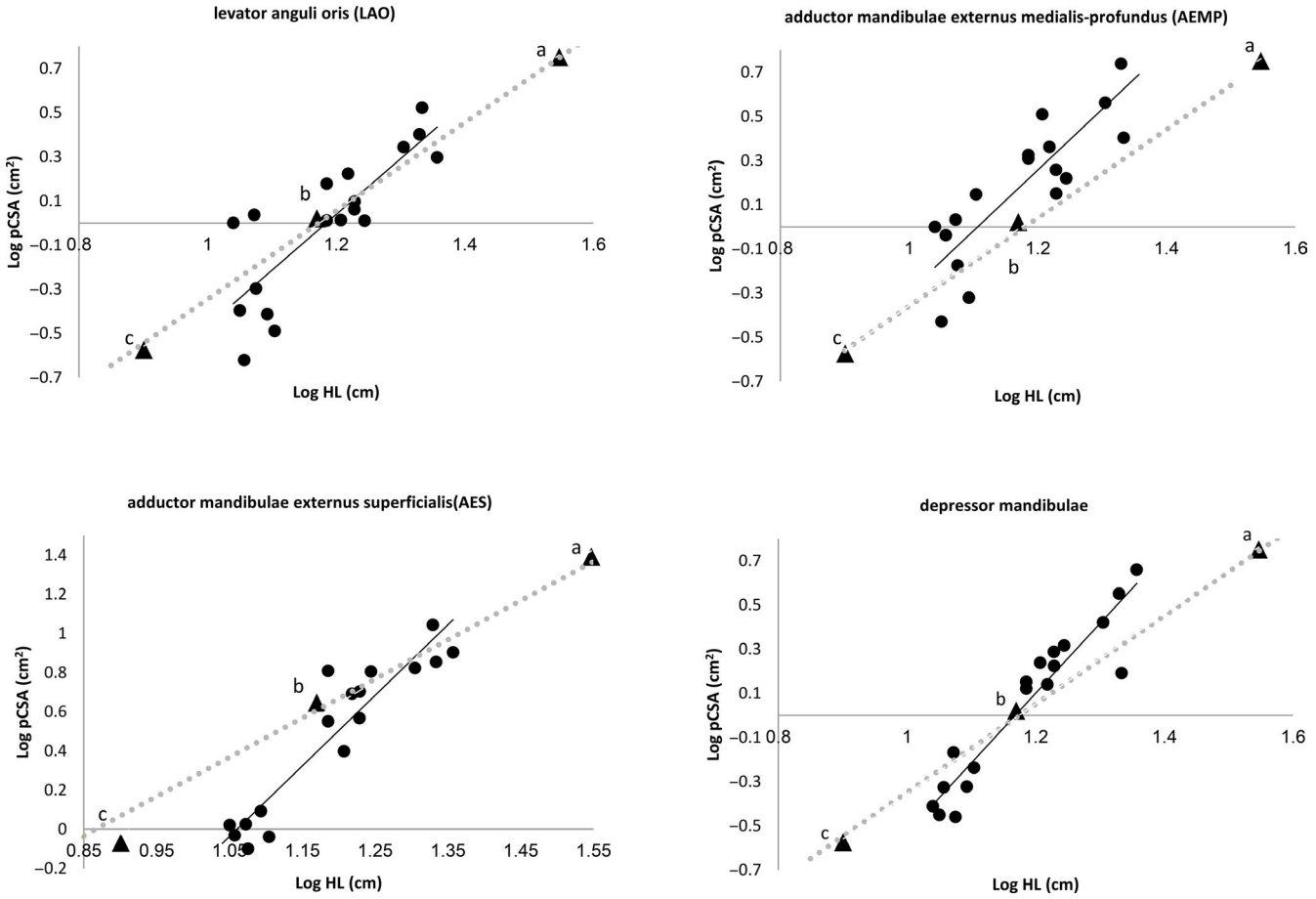

FIGURE 9 The relationships between jaw muscle physiological cross-sectional areas (PCSA) and head length in banded water snakes (*Nerodia fasciata*) (circle) and *Dolichophis–Eirenis* lineage (*E. persicus* (c), *E. punctatolineatus* (b), and *D. schmidti* (a)) (triangle). Continuous line indicates the linear regression line among the *N. fasciata* specimens. Dotted lines indicate the slope predicted under a model of geometric similarity (area = 2). For the abbreviation of muscle names, see Table 2

lineages that show a more or less isometric pattern (slope = 2). Currently, in the ontogenetic series of reptiles studied (Erickson *et al*., 2003; Herrel and O'Reilly, 2005; Herrel *et al*., 2006; Vincent *et al*., 2007; Pfaller *et al*., 2011; Erickson *et al*., 2014; Gignac and Erickson, 2016) positive allometry in feeding muscles and bite force are observed, against either body or head size, indicating that big-sized adults have longer jaw elements and stronger feeding muscles than small size juveniles. Thus, in *Dolichophis–Eirenis* dwarfing lineages, different patterns are observed through miniaturization, indicating that dwarfing in jaw muscles is not simply a truncation of ontogeny but implies novel and unique adaptations that seem to be unrelated to general ontogenetic patterns.

ACKNOWLEDGMENTS

We are grateful to Nasrullah Rastegar Pouyani, Roman Nazarov, Josef Schmidtler, Joachim Christiaens, Hiwa Faizi, Bahman Zangi, and Mohammad Jahan for their kind cooperation. The special research fund of the Ghent University (BOF-UGent) is acknowledged for the financial support of the UGCT Centre of Expertise (BOF.EXP.2017.0007). Mahdi Rajabizadeh thanks the French Embassy in Tehran for a postdoc grant (2018) that allowed him to work at the MNHN in Paris.

ORCID

Mahdi Rajabizadeh https://orcid.org/0000-0002-6661-799X
Dominique Adriaens https://orcid.org/0000-0003-3610-2773
Barbara De Kegel https://orcid.org/0000-0002-4194-234X
Çetin Ilgaz https://orcid.org/0000-0001-7862-9106
Anthony Herrel https://orcid.org/0000-0003-0991-4434

REFERENCES

Anderson, J. (1872) On some Persian, Himalayan, and other reptiles. *Proceedings of the Zoological Society of London*, 2, 371–404.
Bauchot, R. (1978) Encephalization in vertebrates. *Brain, Behavior and Evolution*, 15, 1–18.
Biewener, A.A. (2003) *Animal locomotion*. Oxford: Oxford University Press.
Boback, S.M. and Guyer, C. (2003) Empirical evidence for an optimal body size in snakes. *Evolution*, 57, 345–351.
Boettger, O. (1888) Über die Reptilien und Batrachier Transcaspiens. *Zoologischer Anzeiger*, 11, 259–263.
Boettger, O. (1892) Kriechthiere der Kaukasusländer, gesammelt durch die Radde-Valentin'sche Expedition nach dem Karabagh und

durch die Herren Dr. J. Valentin un P. Reibisch. *Berlin Senckenberg Gesellschaft*, 1892, 131–150.

Brecko, J., Vervust, B., Herrel, A. and Van Damme, R. (2011) Head morphology and diet in the dice snake (*Natrix tessellata*). *Mertensiella*, 18, 20–29.

Bullock, R.E. and Tanner, W.W. (1966) A comparative osteological study of two species of Colubridae: (*Pituophis* and *Thamnophis*). *Brigham Young University Science Bulletin, Biological Series*, 8, 1–28.

Çıçek, K. and Mermer, A. (2007) A Preliminary study of the food of the Dwarf snake, *Eirenis modestus* (Martin, 1838) (Serpentes: Colubridae), in İzmir and Manisa Provinces. *Turkish Journal of Zoology*, 31, 399–402.

Close, M. and Cundall, D. (2014) Snake lower jaw skin: extension and recovery of a hyperextensible keratinized integument. *Journal of Experimental Zoology Part A: Ecological Genetics and Physiology*, 321, 78–97.

Close, M., Perni, S., Franzini-Armstrong, C. and Cundall, D. (2014) Highly extensible skeletal muscle in snakes. *Journal of Experimental Biology*, 217, 2445–2448.

Cundall, D. (1983) Activity of head muscles during feeding by snakes: a comparative study. *American Zoologist*, 23, 383–396.

Cundall, D., Deufel, A., MacGregor, G., Pattishall, A. and Richter, M. (2016) Effects of size, condition, measurer, and time on measurements of snakes. *Herpetologica*, 72, 227–234.

Cundall, D. and Gans, C. (1979) Feeding in water snakes: an electromyographic study. *Journal of Experimental Zoology*, 209, 189–207.

Cundall, D. and Greene, H.W. (2000) *Feeding in snakes. Feeding: form, function, and evolution in tetrapod vertebrates*. Cambridge, MA: Academic Press, 293–333.

Cundall, D., Tuttman, C. and Close, M. (2014) A model of the anterior esophagus in snakes, with functional and developmental implications. *The Anatomical Record*, 297, 586–598.

Das, S. and Pramanick, K. (2019) Comparative anatomy and homology of jaw adductor muscles of some South Asian colubroid snakes (Serpentes: Colubroidea). *Vertebrate Zoology*, 69, 93–102.

Descamps, E., Sochacka, A., De Kegel, B., Van Loo, D., Van Hoorebeke, L. and Adriaens, D. (2014) Soft tissue discrimination with contrast agents using micro-CT scanning. *Belgian Journal of Zoology*, 144(1), 20–40.

Erickson, G., Gignac, P., Lappin, A., Vliet, K., Brueggen, J. and Webb, G. (2014) A comparative analysis of ontogenetic bite-force scaling among Crocodylia. *Journal of Zoology*, 292, 48–55.

Erickson, G.M., Lappin, A.K. and Vliet, K.A. (2003) The ontogeny of bite-force performance in American alligator (*Alligator mississippiensis*). *Journal of Zoology*, 260, 317–327.

Figueroa, A., McKelvy, A.D., Grismer, L.L., Bell, C.D. and Lailvaux, S.P. (2016) A species-level phylogeny of extant snakes with description of a new colubrid subfamily and genus. *PLoS One*, 11, e0161070.

Fitzinger, L. (1843) *Systema reptilium, Fasciculus primus: Amblyglossae (Conspectus Geographicus)*. Vindodonae [Vienna]: Braumuller and Seidel.

Forsman, A. (1996) Body size and net energy gain in gape-limited predators: a model. *Journal of Herpetology*, 30(3), 307–319.

Gignac, P. and Erickson, G. (2016) Ontogenetic bite-force modeling of Alligator mississippiensis: implications for dietary transitions in a large-bodied vertebrate and the evolution of crocodylian feeding. *Journal of Zoology*, 299, 229–238.

Göçmen, B., Werner, Y.L. and Elbeyli, B. (2008) Cannibalism in *Dolichophis jugularis* (Serpentes: Colubridae): more than random? *Current Herpetology*, 27, 1–7.

Hampton, P.M. (2011) Comparison of cranial form and function in association with diet in natricine snakes. *Journal of Morphology*, 272, 1435–1443.

Hampton, P.M. (2014) Allometry of skull morphology, gape size and ingestion performance in the banded watersnake (*Nerodia fasciata*) feeding on two types of prey. *Journal of Experimental Biology*, 217, 472–478.

Hampton, P.M. and Moon, B.R. (2013) Gape size, its morphological basis, and the validity of gape indices in western diamond-backed rattlesnakes (*Crotalus atrox*). *Journal of Morphology*, 274, 194–202.

Hanken, J. (1983) Miniaturization and its effects on cranial morphology in plethodontid salamanders, genus *Thorius* (Amphibia, Plethodontidae): II. The fate of the brain and sense organs and their role in skull morphogenesis and evolution. *Journal of Morphology*, 177, 255–268.

Hanken, J. and Wake, D.B. (1993) Miniaturization of body size: organismal consequences and evolutionary significance. *Annual Review of Ecology and Systematics*, 24, 501–519.

Hedges, S.B. (2008) At the lower size limit in snakes: two new species of threadsnakes (Squamata: Leptotyphlopidae: Leptotyphlops) from the Lesser Antilles. *Zootaxa*, 1841, 1–30.

Herrel, A., Aerts, P. and De Vree, F. (1997) Ecomorphology of the lizard feeding apparatus: a modelling approach. *Netherlands Journal of zoology*, 48, 1–25.

Herrel, A., Aerts, P. and De Vree, D. (1998) Static biting in lizards: functional morphology of the temporal ligaments. *Journal of Zoology*, 244, 135–143.

Herrel, A. and Holanova, V. (2008) Cranial morphology and bite force in Chamaeleolis lizards–adaptations to molluscivory? *Zoology*, 111, 467–475.

Herrel, A., James, R. and Van Damme, R. (2007) Fight versus flight: physiological basis for temperature-dependent behavioral shifts in lizards. *Journal of Experimental Biology*, 210, 1762–1767.

Herrel, A., Joachim, R., Vanhooydonck, B. and Irschick, D.J. (2006) Ecological consequences of ontogenetic changes in head shape and bite performance in the Jamaican lizard *Anolis lineatopus*. *Biological Journal of the Linnean Society*, 89, 443–454.

Herrel, A. and O'Reilly, J.C. (2005) Ontogenetic scaling of bite force in lizards and turtles. *Physiological and Biochemical Zoology*, 79, 31–42.

Jan, G. (1863) *Elenco sistematico degli ofidi descritti e disegnati per l'iconografia generale*. Milano: Lombardi.

Kardong, K. (1986) Kinematics of swallowing in the yellow rat snake, Elaphe obsoleta quadrivittata: a reappraisal. *Japanese Journal of Herpetology*, 11, 96–109.

Kardong, K., Dullemeijer, P. and Fransen, J. (1986) Feeding mechanism in the rattlesnake *Crotalus durissus*. *Amphibia-Reptilia*, 7, 271–302.

King, R. (2002) Predicted and observed maximum prey size–snake size allometry. *Functional Ecology*, 16, 766–772.

Lefebvre, L., Reader, S.M. and Sol, D. (2004) Brains, innovations and evolution in birds and primates. *Brain, Behavior and Evolution*, 63, 233–246.

Legendre, P. (2018) *Package 'lmodel2'*. https://www.rdocumentation.org/packages/lmodel2

Lelièvre, H., Legagneux, P., Blouin-Demers, G., Bonnet, X. and Lourdais, O. (2012) Trophic niche overlap in two syntopic colubrid snakes (*Hierophis viridiflavus* and *Zamenis longissimus*) with contrasted lifestyles. *Amphibia-Reptilia*, 33, 37–44.

Lenk, P., Herrmann, H.-W., Joger, U. and Wink, M. (1999) Phylogeny and taxonomic subdivision of Bitis (Reptilia: Viperidae) based on molecular evidence. *Kaupia*, 8, 31–38.

Mahlow, K., Tillack, F., Schmidtler, J.F. and Müller, J. (2013) An annotated checklist, description and key to the dwarf snakes of the genus *Eirenis* Jan, 1863 (Reptilia: Squamata: Colubridae), with special emphasis on the dentition. *Vertebrate Zoology*, 63, 41–85.

Masschaele, B.C., Cnudde, V., Dierick, M., Jacobs, P., Van Hoorebeke, L. and Vlassenbroeck, J. (2007) UGCT: New X-ray radiography and tomography facility. *Nuclear Instruments and Methods in Physics Research Section A: Accelerators, Spectrometers, Detectors and Associated Equipment*, 580(1), 266–269.

Masschaele, B., Dierick, M., Loo, D.V., Boone, M.N., Brabant, L., Pauwels, E. *et al.* (2013) HECTOR: A 240kV micro-CT setup optimized for research. *Journal of Physics: Conference Series*, 463(1), 012012.

McMahon, T.A. (1984) *Muscles, reflexes, and locomotion*. Princeton, NJ: Princeton University Press.

Miller, D.E. and Mushinsky, H.R. (1990) Foraging ecology and prey size in the mangrove water snake, *Nerodia fasciata* compressicauda. *Copeia*, 1990, 1099–1106.

Moon, B.R., Penning, D.A., Segall, M. and Herrel, A. (2019) *Feeding in snakes: Form, function, and evolution of the feeding system. In feeding in vertebrates*. Cham: Springer, pp. 527–574.

Nagy, Z.T., Schmidtler, J.F., Joger, U. and Wink, M. (2003) Systematik der Zwergnattern (Reptilia: Colubridae: *Eirenis*) und verwandter Gruppen anhand von DNA-Sequenzen und morphologischen Daten. *Salamandra-Bonn*, 39, 149–168.

Nikolsky, A.M. (1909) Novae species reptiliem e Caucaso [in Russian]. *Tiflis Mitteilungen Kaukas Museum*, 4, 301–306.

Pfaller, J.B., Gignac, P.M. and Erickson, G.M. (2011) Ontogenetic changes in jaw-muscle architecture facilitate durophagy in the turtle Sternotherus minor. *Journal of Experimental Biology*, 214, 1655–1667.

Pyron, A.R. and Burbrink, F. (2009) Body size as a primary determinant of ecomorphological diversification and the evolution of mimicry in the lampropeltinine snakes (Serpentes: Colubridae). *Journal of Evolutionary Biology*, 22, 2057–2067.

Pyron, R.A., Burbrink, F.T. and Wiens, J.J. (2013) A phylogeny and revised classification of Squamata, including 4161 species of lizards and snakes. *BMC Evolutionary Biology*, 13, 93.

R Core Team (2014) *R: A language and environment for statistical computing*. Vienna, Austria: R Foundation for Statistical Computing.

Rajabizadeh, M. (2018) *Snake of Iran*. Tehran, Iran: Iranshenasi.

Rajabizadeh, M., Nagy, Z.T., Adriaens, D., Avci, A., Masroor, R., Schmidtler, J. *et al.* (2016) Alpine-Himalayan orogeny drove correlated morphological, molecular, and ecological diversification in the Persian dwarf snake (Squamata: Serpentes: *Eirenis persicus*). *Zoological Journal of the Linnean Society*, 176, 878–913.

Rajabizadeh, M., Schmidtler, J.F., Javanmardi, S., Rastegar-Pouyani, N. and Esmaeili, H.R. (2012) Taxonomy, distribution and geographic variation of *Eirenis punctatolineatus* (Boettger, 1892) (Reptilia: Colubridae). *Amphibia-Reptilia*, 33, 69–82.

Rayner, J.M. (1985) Linear relations in biomechanics: the statistics of scaling functions. *Journal of Zoology*, 206, 415–439.

Revell, L.J. (2012) Package "phytools", phylogenetic tools for comparative biology (and other things). *Methods in Ecology and Evolution*, 3(2), 217–223. https://doi.org/10.1111/j.2041-210X.2011.00169.x

Romer, A.S. (1956) *Osteology of the reptiles*. Chicago: University of Chicago Press.

Roth, G., Blanke, J. and Ohle, M. (1995) Brain size and morphology in miniaturized plethodontid salamanders. *Brain, Behavior and Evolution*, 45, 84–95.

Schaerlaeken, V., Holanova, V., Boistel, R., Aerts, P., Velensky, P., Rehak, I. *et al.* (2012) Built to bite: feeding kinematics, bite forces, and head shape of a specialized durophagous lizard, *Dracaena guianensis* (Teiidae). *Journal of Experimental Zoology Part A: Ecological Genetics and Physiology*, 317, 371–381.

Schätti, B. (1987) The phylogenetic significance of morphological characters in the Holarctic racers of the genus *Coluber* Linnaeus, 1758 (Reptilia, Serpentes). *Amphibia-Reptilia*, 8, 401–415.

Schätti, B. (1988) *Systematik und Evolution der Schlangengattung Hierophis Fitzinger, 1843*. Diss. Univ. Zuerich.

Schätti, B. and Utiger, U. (2001) Hemerophis, a new genus for *Zamenis socotrae* Günther, and a contribution to the phylogeny of Old World racers, whip snakes, and related genera (Reptilia: Squamata: Colubrinae). *Revue suisse de Zoologie*, 108, 919–948.

Schmidt-Nielsen, K. (1984) *Scaling: why is animal size so important?* Cambridge: Cambridge University Press.

Schmidtler, J.F. (1993) Zur Systematik und Phylogenie des Eirenis-modestus-Komplexes in Süd-Anatolien (Serpentes, Colubridae). *Spixiana*, 16, 79–96.

Schmidtler, J.J. and Schmidtler, J.F. (1978) Eine neue Zwergnatter aus der Türkei; mit einer Übersicht über die Gattung Eirenis (Colubridae, Reptilia). *Annalen des Naturhistorischen Museums in Wien*, 81, 383–400.

Schwenk, K. (2000) *Feeding: form, function and evolution in tetrapod vertebrates*. Cambridge, MA: Academic Press.

Shwayat, S.N., Disi, A.M. and Amr, Z.S. (2009) Snakes of the genus *Eirenis* in Jordan (Reptilia: Squamata: Colubridae). *Vertebrate Zoology*, 59, 91–101.

Sol, D., Bacher, S., Reader, S.M. and Lefebvre, L. (2008) Brain size predicts the success of mammal species introduced into novel environments. *The American Naturalist*, 172, S63–S71.

Striedter, G. (2005) *Principles of brain evolution*. Sunderland, MA: Sinauer.

Taskinen, S. and Warton, D. (2013) Robust tests for one or more allometric lines. *Journal of Theoretical Biology*, 333, 38–46.

Terent év, P.V. and Chernov, S.A. (1965) *Key to amphibian and reptiles, Program for Scientific translation [English translation of Terent év & Chernov, 1949]*. Jerusalem, Israel.

Venchi, A. and Sindaco, R. (2006) Annotated checklist of the reptiles of the Mediterranean countries, with keys to species identification. Part 2-Snakes (Reptilia, Serpentes). *Annali del Museo Civico di Storia Naturale*, 98, 259–364.

Vincent, S., Brandley, M., Kuriyama, T., Mori, A., Herrel, A. and Hasegawa, M. (2009) Insular gigantism and dwarfism in a snake, adaptive response or spandrel to selection on gape size. *Nature Precedings*, hdl, 10101.

Vincent, S., Moon, B., Shine, R. and Herrel, A. (2006) The functional meaning of "prey size" in water snakes (*Nerodia fasciata*, Colubridae). *Oecologia*, 147, 204–211.

Vincent, S.E., Moon, B.R., Herrel, A. and Kley, N.J. (2007) Are ontogenetic shifts in diet linked to shifts in feeding mechanics? Scaling of the feeding apparatus in the banded watersnake *Nerodia fasciata*. *Journal of Experimental Biology*, 210, 2057–2069.

Vlassenbroeck, J., Dierick, M., Masschaele, B., Cnudde, V., Van Hoorebeke, L. and Jacobs, P. (2007) Software tools for quantification of X-ray microtomography at the UGCT. *Nuclear Instruments and Methods in Physics Research Section A: Accelerators, Spectrometers, Detectors and Associated Equipment*, 580, 442–445.

Warton, D.I., Duursma, R.A., Falster, D.S. and Taskinen, S. (2012) smatr 3–an R package for estimation and inference about allometric lines. *Methods in Ecology and Evolution*, 3, 257–259.

Weston, E.M. and Lister, A.M. (2009) Insular dwarfism in hippos and a model for brain size reduction in *Homo floresiensis*. *Nature*, 459, 85–88.

Wilson, L.D. and Mata-Silva, V. (2014) Snakes of the genus *Tantilla* (Squamata: Colubridae) in Mexico: taxonomy, distribution, and conservation. *Mesoamerican Herpetology*, 1, 1–95.

Yeh, J. (2002) The effect of miniaturized body size on skeletal morphology in frogs. *Evolution*, 56, 628–641.

Zaher, H., Murphy, R.W., Arredondo, J.C., Graboski, R., Machado-Filho, P.R., Mahlow, K. *et al.* (2019) Large-scale molecular phylogeny, morphology, divergence-time estimation, and the fossil record of advanced caenophidian snakes (Squamata: Serpentes). *PLoS One*, 14, e0216148.

Zimkus, B.M., Lawson, L., Loader, S.P. and Hanken, J. (2012) Terrestrialization, miniaturization and rates of diversification in African puddle frogs (Anura: Phrynobatrachidae). *PLoS One*, 7, e35118.

SUPPORTING INFORMATION

Additional supporting information may be found online in the Supporting Information section.

How to cite this article: Rajabizadeh M, Adriaens D, De Kegel B, Avcı A, Ilgaz Ç, Herrel A. Body size miniaturization in a lineage of colubrid snakes: Implications for cranial anatomy. *J. Anat.* 2020;00:1–15. https://doi.org/10.1111/joa.13293